Journal of Chromatography A, 1217 (2010) 7942–7948

Contents lists available at ScienceDirect

Journal of Chromatography A

journal homepage: www.elsevier.com/locate/chroma

Enantioselective capillary electrophoresis for identification and characterization of human cytochrome P450 enzymes which metabolize ketamine and norketamine *in vitro*

Simone Portmann[a], Hiu Ying Kwan[a], Regula Theurillat[a], Andrea Schmitz[b], Meike Mevissen[b], Wolfgang Thormann[a,*]

[a] Department of Clinical Pharmacology and Visceral Research, University of Bern, Murtenstrasse 35, CH-3010 Bern, Switzerland
[b] Division of Veterinary Pharmacology and Toxicology, Vetsuisse Faculty, University of Bern, Bern, Switzerland

ARTICLE INFO

Article history:
Available online 16 June 2010

Keywords:
Capillary electrophoresis
Ketamine
Norketamine
CYP3A4
CYP2A6
CYP2B6
Pharmacokinetics
Stereoselective metabolism

ABSTRACT

Ketamine, a phencyclidine derivative, is used for induction of anesthesia, as an anesthetic drug for short term surgical interventions and in subanesthetic doses for postoperative pain relief. Ketamine undergoes extensive hepatic first-pass metabolism. Enantioselective capillary electrophoresis with multiple isomer sulfated β-cyclodextrin as chiral selector was used to identify cytochrome P450 enzymes involved in hepatic ketamine and norketamine biotransformation *in vitro*. The N-demethylation of ketamine to norketamine and subsequently the biotransformation of norketamine to other metabolites were studied via analysis of alkaline extracts of *in vitro* incubations of racemic ketamine and racemic norketamine with nine recombinantly expressed human cytochrome P450 enzymes and human liver microsomes. Norketamine was formed by CYP3A4, CYP2C19, CYP2B6, CYP2A6, CYP2D6 and CYP2C9, whereas CYP2B6 and CYP2A6 were identified to be the only enzymes which enable the hydroxylation of norketamine. The latter two enzymes produced metabolic patterns similar to those found in incubations with human liver microsomes. The kinetic data of ketamine N-demethylation with CYP3A4 and CYP2B6 were best described with the Michaelis–Menten model and the Hill equation, respectively. This is the first study elucidating the individual enzymes responsible for hydroxylation of norketamine. The obtained data suggest that *in vitro* biotransformation of ketamine and norketamine is stereoselective.

1. Introduction

Ketamine ((R,S-2-(2-chlorophenyl)-2-methylamino)cyclohexanon, for chemical structure see Fig. 1), is a phencyclidine derivative that is used in human and veterinary clinical practice since 1970. Ketamine's mechanism of action has not been fully elucidated yet, but it is considered that the most important neuropharmacological effects of ketamine are mediated through its non-competitive antagonism at the N-methyl-D-aspartate (NMDA) receptor. Interactions of ketamine with opioid receptors, muscarinic acetylcholine receptors and different voltage-gated channels have been described. Because of rapid onset and short duration of action, ketamine is frequently used for induction of anesthesia and for short term surgical procedures. Due to its hallucinogenic effects even at subanesthetic doses it is abused by medical personnel and ketamine (also known as special K) became popular among the European party scenes as a drug of abuse where it is taken intranasally, injected, smoked, or ingested as part of a drink. Ketamine consists of a racemic mixture of two enantiomers, S-ketamine and R-ketamine. The S-enantiomer has a four times higher affinity for the NMDA receptor than the R-enantiomer and also binds to the μ and κ opioid receptors. The anesthetic potency of S-ketamine is two to three times higher than that of the racemic mixture. The incidence of unwanted side-effects at equal plasma concentrations is identical for both enantiomers, but since lower doses of the S-enantiomer are needed to maintain an equal state of anesthesia, fewer side-effects and shorter recovery times are seen with the single enantiomer preparation. The pK_a value of ketamine is 7.5 and it is therefore positively charged at physiological pH. The partition coefficient, also named the log *P* (octanol/water) value, accounts for 3.1. Due to its high lipid solubility and low protein binding (20–50% is bound to plasma proteins), ketamine is extensively distributed throughout the body. The half-life of the parent compound has been reported to be about 3 h and it can be administered intravenously, intramuscularly, orally, rectally, subcutaneously, epidurally and on the transnasal route [1–8].

* Corresponding author. Tel.: +41 31 632 3288; fax: +41 31 632 4997.
E-mail address: wolfgang.thormann@ikp.unibe.ch (W. Thormann).

0021-9673/$ – see front matter © 2010 Elsevier B.V. All rights reserved.
doi:10.1016/j.chroma.2010.06.028

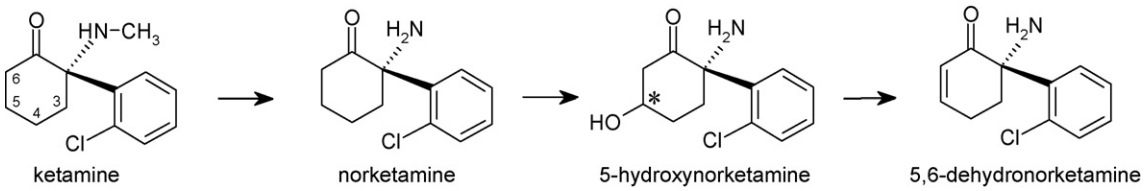

Fig. 1. Chemical structures for S-ketamine, S-norketamine, 5-hydroxynorketamine and S-5,6-dehydronorketamine. The asterisk marks the formation of a carbon stereogenic center which is formed upon hydroxylation of norketamine at the cyclohexanone ring.

The metabolism of ketamine has been studied in humans and various animal species. It was found that ketamine, incubated with human liver microsomes (HLM), is metabolized by the hepatic cytochrome P450 (CYP) enzyme system through N-demethylation to norketamine followed by hydroxylation of norketamine at various locations at the cyclohexanone and chlorophenyl rings and the formation of 5,6-dehydronorketamine [8–14]. The major metabolic phase I pathway for S-ketamine is depicted in Fig. 1. Direct hydroxylation of ketamine prior to N-demethylation is also possible but occurs to a marginal extent. The same metabolites are observed for other species *in vitro* [14–17], as well as *in vivo* in humans and animals [15,18–23].

The pharmacological activities of the metabolites have not been well studied in humans. In view of the growing interest concerning ketamine as a therapeutic agent and a drug of abuse, knowledge of the metabolism of ketamine in humans and the involved cytochrome P450 enzymes is of importance. Previous studies with lymphoblast-expressed CYP enzymes evidenced that CYP3A4, CYP2B6 and CYP2C9 are mainly responsible for the biotransformation of ketamine to its active metabolite norketamine [11,12]. Furthermore, incubation of the two ketamine enantiomers with 12 single CYP enzymes revealed also N-demethylation activities for CYP2A6, CYP2C8, CYP2C19 and CYP2D6 [11]. *In vitro* studies with individual enzymes concerning metabolites other than norketamine could not be found in the literature. Thus, efforts in elucidating the CYP enzymes involved in the metabolism of ketamine and norketamine were undertaken. In addition the stereoselectivity of each metabolic pathway was investigated. This work was executed in the context of a multidisciplinary research cooperation elucidating the metabolism and the pharmacokinetics of ketamine in different species. The project includes studies *in vitro* [14,15,17,24] and *in vivo* [15,22,23,25–29] for which enantioselective capillary electrophoresis (CE) with multiple isomer sulfated β-cyclodextrin (β-CD) as chiral selector [15,22,23] was employed to analyze the stereoisomers of ketamine and its metabolites in equine, canine and human biosamples.

The main goal of this project was to identify human CYP enzymes which are involved in the biotransformation of ketamine to norketamine *in vitro* and to elucidate which of these enzymes catalyze the formation of further metabolites. Individual recombinant human CYP enzymes from a baculovirus expression system (referred to as SUPERSOMES) were used for that task. Special emphasis was put on the stereoselective aspect of ketamine biotransformation by using enantioselective CE for detection of analytes. Racemic ketamine and norketamine were incubated with CYP1A1, CYP1A2, CYP2A6, CYP2B6, CYP2C9, CYP2C19, CYP2D6, CYP3A4 and CYP2E1 SUPERSOMES, and data were compared to those obtained with incubation of the same compounds with HLM and human liver cytosol. Furthermore, the kinetics of ketamine to norketamine N-demethylation were examined for CYP3A4 and CYP2B6 and compared to those obtained with HLM. Two kinetic models (Michaelis–Menten and Hill) were fitted to the experimental data.

2. Materials and methods

2.1. Chemicals, reagents and solutions

Racemic ketamine hydrochloride was obtained from the pharmacy of the Inselspital (Bern, Switzerland). Norketamine as hydrochloride solution in methanol (1 mg/mL of the free base) was purchased from Cerilliant (Round Rock, USA) and (+)-pseudoephedrine hydrochloride was from Fluka (Buchs, Switzerland). Sulfated β-CD (7–11 mol sulfate/mol β-CD) was obtained from Sigma–Aldrich Chemie (Schnelldorf, Germany). Tris and HCl (37%) were from Merck (Darmstadt, Germany), H_3PO_4 (85%), ethylacetate and diammonium hydrogenphosphate from Fluka (Buchs, Switzerland), and dichloromethane from Biosolve (Valkenswaard, The Netherlands). Calibrator and control samples used for quantification of ketamine and norketamine enantiomers were prepared in 100 mM phosphate buffer (pH 7.4).

Baculovirus-insect-cell-expressed human CYP3A4 + P450 reductase + cytochrome b5 SUPERSOMES™, human CYP2C19 + P450 reductase + cytochrome b5 SUPERSOMES™, human CYP2D6*1 + P450 reductase SUPERSOMES™, human CYP1A1 + P450 reductase SUPERSOMES™, human CYP1A2 + P450 reductase SUPERSOMES™, human CYP2C9*1 (Arg_{144}) + P450 reductase + cytochrome b5 SUPERSOMES™, human CYP2B6 + P450 reductase + cytochrome b5 SUPERSOMES™, human CYP2A6 + P450 reductase + cytochrome b5 SUPERSOMES™, and human CYP2E1 + P450 reductase + cytochrome b5 SUPERSOMES™ were purchased from Gentest (Woburn, MA, USA, distributed through Anawa Trading, Wangen, Switzerland). The mixed gender pool of HLM, containing CYP1A2, CYP2A6, CYP2B6, CYP2C8, CYP2C9, CYP2C19, CYP2D6, CYP2E1, CYP3A4, CYP4A and flavin monooxygenase (FMO), with a protein concentration of 20 mg/mL in 250 mM sucrose, pooled human liver cytosol and the nicotinamide adenine dinucleotide phosphate (NADPH) regenerating system were also from Gentest. The regenerating system comprises two solutions, solution A composed of 31.0 mM $NADP^+$, 66 mM glucose-6-phosphate (G-6-P) and 66 mM $MgCl_2$ and solution B containing 40 U/mL glucose-6-phophate dehydrogenase in 5 mM sodium citrate. The microsomes were stored in aliquots at −80 °C and the NADPH regenerating system was kept at −18 °C until use.

2.2. In vitro reactions and sample preparation for metabolic studies

A mixture containing substrate (either 50 μM racemic ketamine or 50 μM racemic norketamine) and NADPH regenerating system (1.55 mM $NADP^+$, 3.3 mM G-6-P, 0.4 U/mL G-6-P dehydrogenase, 3.3 mM $MgCl_2$) in 100 mM potassium phosphate buffer (pH 7.4) was preincubated at 37 °C for 3 min. In case of CYP2C9, a 100 mM Tris buffer (pH 7.5) was used instead of the phosphate buffer. For most CYP enzymes (1A1, 1A2, 3A4, 2C19, 2D6 and 2C9 with CYP content of 1000 pmol/mL), the enzymatic reaction was started at 37 °C after addition of a 16.3 μL aliquot of SUPERSOMES to a 760 μL reaction solution, which provided microsomal incubation mixtures

comprising 21 pmol CYP/mL. For CYP2E1, which has twice the CYP content compared to the other SUPERSOMES used, the microsomal solution was diluted two-fold prior to addition of 16.3 μL of the diluted solution. Aliquots of 200 μL were withdrawn from the reaction mixture after 0, 60 and 120 min of incubation and immediately mixed with 500 μL sodium hydroxide (0.2 M) and 30 μL of the internal standard solution (30 μg/mL (+)-pseudoephedrine hydrochloride). For CYP2B6, CYP2A6, HLM and cytosol, the reaction was commenced with 32.5 μL of SUPERSOMES, HLM or cytosol added to 1510 μL reaction solution and aliquots of 200 μL were withdrawn from the reaction mixture after 0, 60, 120 and 180 min of incubation. All experiments were performed in duplicates. For extraction, 5 mL of a dichloromethane/ethylacetate (75:25%, v/v) solvent mixture was added to the sample. The tubes were closed, shaken for 10 min and centrifuged at about 3500 × *g* for 5 min. The upper aqueous phase and the protein aggregates were removed with a glass pipette under vacuum and the organic phase was decanted into a rounded bottom tube. After acidification with a drop of hydrochloric acid (37%), the organic solvent was evaporated under a stream of air at about 40 °C. Residues from the evaporation were dissolved in 200 μL methanol and vortexed. After evaporation, the residues were redissolved in 30 μL of 5 mM Tris–phosphate buffer (pH 2.5).

2.3. In vitro reactions and sample preparation for kinetic studies

For the characterization of the ketamine N-demethylation with individual CYPs, kinetic studies were performed with 10 substrate concentrations of racemic ketamine ranging from 5 to 1000 μM. The CYP content was 24 pmol/mL, the incubation time was 8 min and the final volume was 200 μL. Linearity of the norketamine formation rate was established previously with respect to microsomal protein and incubation time [14,17]. After incubation, enzymatic reactions were stopped by adding 500 μL sodium hydroxide (0.2 M) to the sample. 50 μL of the internal standard solution was added prior to extraction. All experiments were performed in duplicates. For the extraction, 3 mL of dichloromethane/ethylacetate (75:25%, v/v) was added to the sample. The closed tubes were shaken for 10 min and centrifuged at about 3500 × *g* for 5 min. The upper aqueous phase and the protein aggregates were removed and the organic phase was decanted into a rounded bottom tube. After acidification with a drop of 50 mM phosphoric acid (phosphoric acid was used instead of HCL to prevent corrosion of the water bath), the organic solvent was evaporated under a stream of air at about 45 °C. Residues were dissolved in 200 μL methanol and vortexed, evaporated to dryness and redissolved in 50 μL of 5 mM Tris–phosphate buffer (pH 2.5).

2.4. CE instrumentation and analytical conditions

A Proteome Lab PA 800 instrument or a P/ACE MDQ capillary electrophoretic system (both Beckman Coulter, Fullerton, CA, USA) equipped with a 50 μm ID fused-silica capillary (Polymicro Technologies) of 45 cm total length (effective length of 34 cm) was used. Samples were introduced from 0.5 mL polypropylene vials by applying a vacuum of 1.0 psi (1 psi = 6894.8 Pa) for 7 s (metabolic pattern) or for 6 s (kinetic study). The applied voltages were −17.0 kV (reversed polarity, current about −35 μA) and −20 kV (about −45 μA), respectively. The temperature of the circulating cooling fluid in the capillary cartridge and around sample trays was set to 20 °C. A positive pressure of 0.1 psi to induce a buffer flow towards the anode was applied during the entire run. An on-column UV variable wavelength detector set to 195 nm was employed for analyte detection. The running buffer was composed of 35 mM (metabolic pattern) and 50 mM (kinetic study) Tris, phosphoric acid (pH 2.5) and 10 mg/mL of sulfated β-CD (70%/30%

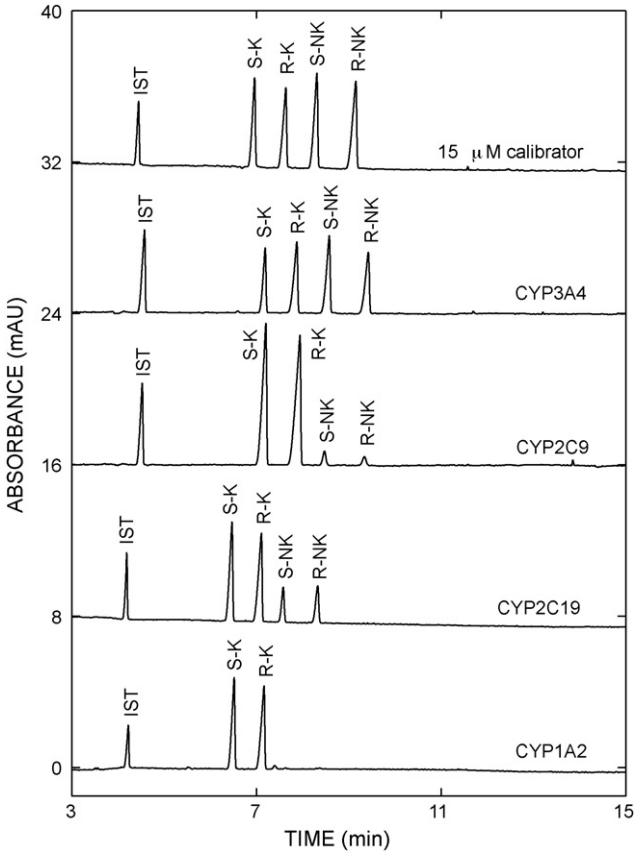

Fig. 2. Electropherograms obtained after a 2 h incubation of selected single CYP enzymes with 50 μM racemic ketamine and a calibrator sample containing 15 μM of each ketamine and norketamine enantiomer. For presentation purposes, data are plotted with a *y*-scale offset of 8 mAU. Key: S-K, S-ketamine; R-K, R-ketamine; S-NK, S-norketamine; R-NK, R-norketamine; IST, internal standard.

blend of batches 13112JD and 13307MA). Fresh buffer was prepared every day. Before each experiment, the capillary was sequentially rinsed with 0.1 M NaOH (2 min, 20 psi), bidistilled water (1 min, 20 psi) and running buffer (1 min, 20 psi). Quantitation of ketamine and norketamine enantiomers was based upon internal calibration using corrected peak areas (areas divided by detection time). Aqueous calibrators containing 0.5, 2.5, 7.5, 15.0 and 30.0 μM of each enantiomer were employed as described previously [14]. A typical electropherogram obtained with a calibrator sample is shown as top graph in Fig. 2. Assay specifications were the same as reported by Schmitz et al. [14,17]. Small differences of the chiral selector concentration in the running buffer resulted in appreciable differences in detection times from day to day (Fig. 2). Based on the internal calibration used and frequent renewal of the calibration data, however, these variations did not have an impact on quantitation.

2.5. Data analysis

Initial enantiomer substrate concentration against the norketamine formation rate (pmol norketamine/min/pmol CYP) was plotted and analyzed by two mathematical models (Michaelis–Menten and Hill) using nonlinear least square regression analysis on the Graph Pad Prism 4 software (Graph Pad Software, San Diego, USA) and SigmaPlot version 10.0 (SPSS, Chicago, IL, USA). Curves were compared between enantiomers with a paired Student's *t*-test using Microsoft Excel software (Microsoft, Seattle, USA). A *p*-value <0.05 was considered significant.

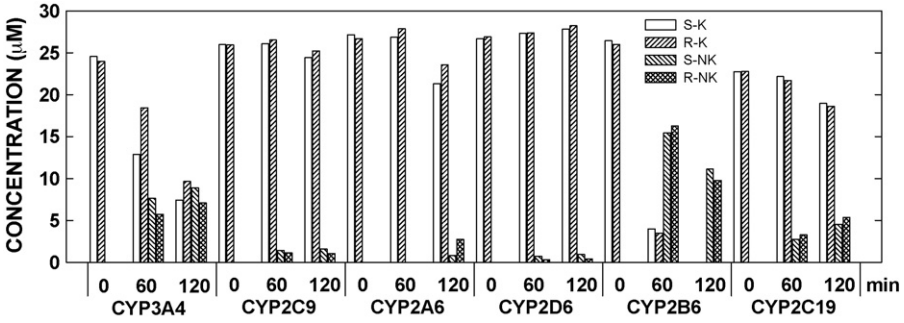

Fig. 3. Ketamine demethylation data of single CYP enzymes for incubations with 50 μM racemic ketamine after 0, 60 and 120 min of incubation time. Key: S-K, S-ketamine; R-K, R-ketamine; S-NK, S-norketamine; R-NK, R-norketamine.

3. Results and discussion

3.1. Identification of enzymes catalyzing N-demethylation of ketamine

Screening of nine human CYP enzymes for ketamine N-demethylation was performed in 2-h incubations using 50 μM racemic ketamine. Samples withdrawn at 0, 60 and 120 min were analyzed be enantioselective CE using a 35 mM Tris–phosphate buffer (pH 2.5) containing 10 mg/mL of sulfated β-CD as a mixture from two different lots. Selected electropherograms are presented in Fig. 2 and N-demethylation results are summarized in Fig. 3. The data reveal that CYP3A4, CYP2C9, CYP2A6, CYP2D6, CYP2B6 and CYP2C19 are responsible for norketamine formation. Norketamine was not detected in the samples comprising CYP1A2, CYP1A1, CYP2E1 and human liver cytosol instead of a CYP (bottom graph in Fig. 2, other data not shown). Quantitation of the enantiomers of ketamine and norketamine was accomplished as described previously for HLM and liver microsomes of other species [14].

The data presented in Fig. 3 suggest that highest demethylation activity is obtained with CYP2B6, followed by CYP3A4, CYP2C19, CYP2A6, CYP2C9 and CYP2D6. Similarly, Yanagihara et al. [11] reported ketamine N-demethylation activities in microsomes from human B-lymphoblastoid cell lines expressing the same six enzymes and CYP2C8, CYP2E1 and CYP1A1, whereas no responses were observed for CYP1A2, CYP1B1 and CYP4A11. Among the CYP enzymes tested, only CYP2B6, CYP3A4 and CYP2C9 showed high activities, whereas the responses with the other enzymes were small with those of CYP2E1 and CYP1A1 being the smallest. Furthermore, Hijazi and Boulieu [12] reported that lymphoblast-expressed CYP2B6 showed higher demethylation activity than CYP3A4 and CYP2C9 which is in agreement with the Yanagihara et al. [11] data for the same three enzymes. Our data were generated with individual baculovirus cDNA-expressed human CYP enzymes. Compared to the behavior of the lymphoblast-expressed enzymes reported in the literature, a higher activity of CYP2C19 compared to that of CYP2C9 was observed. Otherwise, qualitative agreement was noted between the two systems. The fact that CYP1A1 and CYP2E1 did not reveal any activity does not make a significant difference as the activities reported by Yanagihara et al. [11] were very small. Lack of analytical sensitivity of the CE assay used in our work could be responsible for this difference.

The data presented in Figs. 2 and 3 suggest that ketamine is demethylated in a stereoselective manner. Electropherograms obtained after metabolism of ketamine in the presence of single CYP enzymes reveal apparent stereoselectivities. This is particularly obvious for CYP3A4 when its electropherogram (second graph from top in Fig. 2) is compared to that of a calibrator sample in which equal amounts of the enantiomers are present (top graph in Fig. 2). For CE analysis of racemic mixtures, the first detected enantiomer peak is higher compared to the second (top graph in Fig. 2). For the CYP3A4 data, the peak for S-ketamine is smaller than that of R-ketamine which indicates that S-ketamine is faster metabolized compared to R-ketamine. The same is true for the quantitative data presented in Fig. 3. Furthermore, data obtained with CYP2B6 revealed the formation of other peaks that could be related to metabolites of norketamine (cf. Section 3.2). Norketamine peaks at 120 min are smaller compared to those at 60 min suggesting that further metabolites are formed from norketamine (Fig. 3). Similarly, incubation of ketamine with HLM revealed the presence of norketamine and four of its metabolites, as previously described [14].

3.2. Identification of enzymes catalyzing the formation of norketamine metabolites

Incubation of 50 μM racemic norketamine with the nine SUPERSOMES revealed the CYP enzymes involved in the formation of norketamine metabolites. Analysis of the samples was done in the same way as for the incubations of ketamine. Selected electropherograms are presented in Fig. 4. The data revealed that norketamine metabolites are formed by CYP2A6 and CYP2B6. No norketamine metabolites were detected by enantioselective CE for CYP3A4, CYP2C9, CYP2C19, CYP2D6, CYP1A1, CYP1A2 and CYP2E1 (Fig. 4, depicting data for CYP3A4 only).

The obtained electropherograms monitored for the incubations with CYP2B6 and CYP2A6 revealed peaks for the stereoisomers of norketamine, 5,6-dehydronorketamine and three hydroxylated norketamine metabolites with hydroxylation at the cyclohexanone ring as shown in Fig. 4. The enantiomers of 5,6-dehydronorketamine were identified as described in [23], whereas hydroxylated norketamine metabolite peaks (peaks I, III and IV in Fig. 4) were identified as described in [15]. Identification of the metabolites occurred via spiking with standards which were extracted from pony urine and characterized by LC–MS and LC–MS^n [15,23]. All peaks labeled with the prefixes S and R stem from S-norketamine and R-norketamine, respectively. In previous work from our laboratory working with *in vivo* and *in vitro* samples of equines [15], it could be concluded that compounds I and III are precursors of 5,6-dehydronorketamine. Furthermore, because Woolf and Adams [9] did not observe the formation of 5,6-dehydronorketamine in incubations of 6-hydroxynorketamine with HLM, it could be assumed that hydroxynorketamine compounds I and III represent stereoisomers of 5-hydroxynorketamine. The data presented here are in agreement with this assumption. 5,6-Dehydronorketamine is detected in the experiments with CYP2B6 in which hydoxynorketamine compounds III and I were found (center graph of Fig. 4). The data obtained with CYP2A6 did

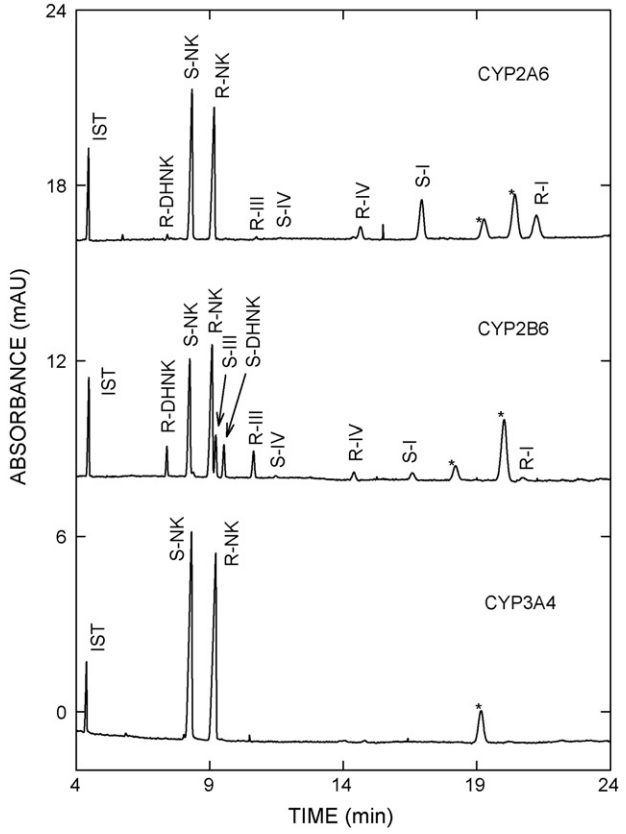

Fig. 4. Electropherograms obtained after a 2 h incubation of selected single CYP enzymes with 50 μM racemic norketamine. For presentation purposes, data are plotted with a *y*-scale offset of 8 mAU. Asterisks mark peaks that are unrelated to norketamine metabolites. Key: S-NK, S-norketamine; R-NK, R-norketamine; S-DHNK, S-5,6-dehydronorketamine; R-DHNK, R-5,6-dehydronorketamine; I, III and IV; hydroxylated norketamine metabolites; IST, internal standard.

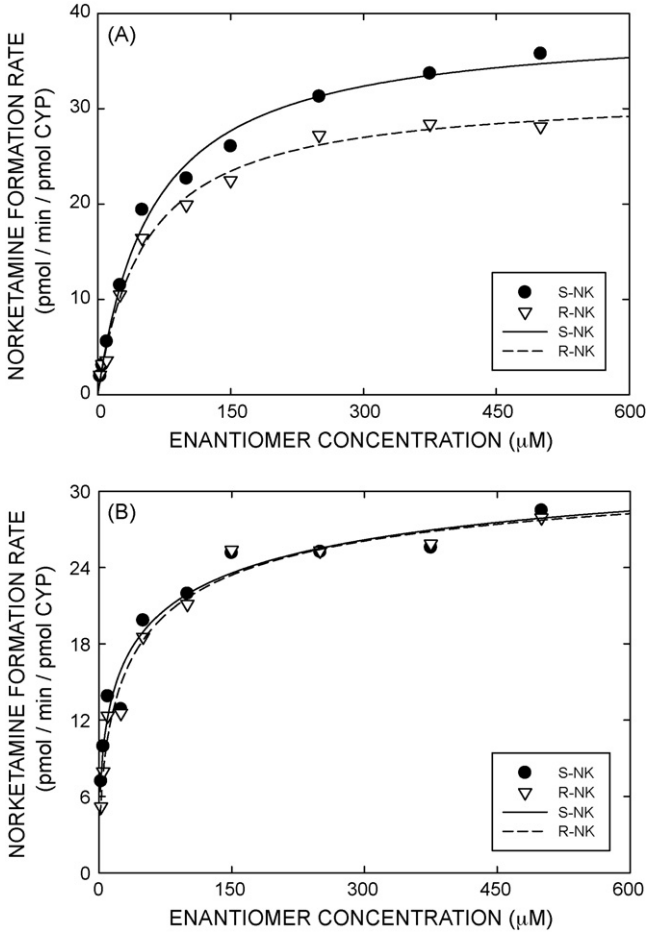

Fig. 5. Enantioselective kinetics of norketamine formation by (A) CYP3A4 and (B) CYP2B6. Racemic ketamine was incubated for 8 min with 24 pmol CYP/mL reaction mixture and norketamine formed was quantitated by enantioselective capillary electrophoresis. Symbols denote the mean of duplicates. Solid and dotted lines are predicted values based on nonlinear regression analysis using (A) the Michaelis–Menten equation and (B) the Hill equation. Key: (●) S-norketamine (S-NK) and (▽) R-norketamine (R-NK).

reveal a significant amount of compound I but almost no compound III (tiny peak for R-III only) and a small amount of R-DHNK (top graph of Fig. 4). This suggests that compound III is more likely to be converted into 5,6-dehydronorketamine. Without having standards of these compounds, however, absolute proof cannot be obtained. As discussed previously, compound IV is most likely (Z)-6-hydroxynorketamine [15]. The formation of compound II (tentatively assigned to 4-hydroxynorketamine), which was found in *in vivo* samples of equines [15] and possibly also *in vitro* with HLM [14], was not observed in the experiments with the two individual CYP enzymes. Compounds I, III and IV are identical to those found in incubations of ketamine with liver microsomes of humans, cats and horses [14] and in incubations of norketamine with HLM (data not shown).

Incubation of CYP2B6 with racemic norketamine revealed that S-norketamine was metabolized faster than R-norketamine (center graph of Fig. 4). This difference was not observed with CYP2A6 (top graph of Fig. 4). However, it is apparent that hydroxylated norketamine metabolites and 5,6-dehydronorketamine is formed in a stereoselective manner. The specific content of individual CYP450 isoforms in HLM vary strongly. Relative amounts of the CYP2A6, CYP2B6 and CYP3A4 enzymes are reported to be 4.0, 0.2 and 28.8%, respectively [30]. Thus, it was interesting to find that norketamine is only metabolized by two CYP enzymes which have a low abundance (total of 4.2% of CYP content in liver microsomes). To the contrary, ketamine is demethylated by CYP enzymes whose total CYP content in liver microsomes approximates 53%.

3.3. Characterization of N-demethylation kinetics of ketamine

For CYP2B6 and CYP3A4, the two enzymes with highest demethylation activity (Fig. 3), the demethylation kinetics were assessed via determination of the norketamine formation rate as function of substrate concentration using an incubation time interval of 8 min. Preliminary experiments revealed that an 8 min incubation was within the linear range of norketamine formation and did not produce any detectable metabolites of norketamine. Racemic ketamine was applied and the ketamine enantiomer concentration was varied between 2.5 and 500 μM. The concentrations of the norketamine enantiomers were determined by enantioselective CE and their formation rates were calculated in relation to the incubation time and the amount of CYP enzyme involved. Data are presented in Fig. 5 and were evaluated according to the Michaelis–Menten and Hill kinetic models. The single site Michaelis–Menten model is based on:

$$v = \frac{V_{max}[S]}{K_m + [S]} \quad (1)$$

whereas the Hill equation is expressed by

$$v = \frac{V_{max}[S]^n}{(K'^n + [S]^n)} \quad (2)$$

Table 1
Kinetic parameters for N-demethylation of ketamine and model comparison[a].

Enzyme system	Product	Michaelis–Menten model				Hill model					F-test [f]
		R^2	K_m [μM]	V_{max} [pmol/min/pmol CYP]	CL_{int} [b] [μL/min/pmol CYP]	R^2	K' [c] [μM]	V_{max} [pmol/min/pmol CYP]	CL_{max} [d] [μL/min/pmol CYP]	n [e]	p-Value
CYP3A4	S-NK	0.9934	61.18	38.95	0.64	0.9951	76.27	42.21	0.87	0.8676	0.1644
CYP3A4	R-NK	0.9929	53.36	31.79	0.60	0.9929	53.79	31.89	0.62	0.9930	0.9501
CYP2B6	S-NK	0.8957	11.89	26.25	2.21	0.9639	43.08	36.60	3.65	0.4743	0.0083
CYP2B6	R-NK	0.9423	17.61	27.01	1.53	0.9773	37.38	33.66	2.81	0.5937	0.0135
HLM	S-NK	0.9705	62.80	13.41	0.21	0.9742	80.76	14.52	0.32	0.8194	0.3536
HLM	R-NK	0.9703	69.58	12.64	0.18	0.9723	83.60	13.42	0.26	0.8619	0.5132

[a] Data for incubation of racemic ketamine derived from mean values of duplicate determinations.
[b] $CL_{int} = V_{max}/K_m$.
[c] K' is equivalent to K_m when $n = 1$.
[d] $Cl_{max} = (V_{max}/K') [(n-1)/n(n-1)^{1/n}]$.
[e] n = Hill coefficient.
[f] Model comparison.

where v is the product formation rate (velocity) of the metabolic reaction, [S] is the substrate concentration, K_m is the Michaelis–Menten constant which is the concentration at which the formation rate is 50% of V_{max}, V_{max} is the maximum formation rate, K' is a constant of the autoactivation model which is equivalent to K_m when $n = 1$, and n is the Hill coefficient [17,31,32]. Standard parameters such as regression coefficient (R^2) and F-test were used to determine the quality of a fit to a specific model. For model comparison with the F-test, $p < 0.05$ means that the alternative model (Hill model) fits the data significantly better. The determined parameters are summarized in Table 1. For the experiment with CYP3A4, the Hill equation (Eq. (2)) did not provide a better fit to the experimental data ($p > 0.05$, Table 1), indicating that autoactivation does not take place. No difference was found for the correlation coefficients (R^2) and n values were determined to be close to unity (Table 1). Thus, the experimental data can best be described with the Michaelis–Menten model (Eq. (1)). For the kinetics of S- and R-ketamine N-demethylation, significant differences between K_m and V_{max} values were observed with both values being higher for the formation of S-norketamine compared to R-norketamine (Table 1). The two curves were found to differ significantly ($p = 0.004$). Thus, the conclusion can be drawn that the demethylation of ketamine via CYP3A4 occurs stereoselectively. For the experiment with CYP2B6 the Hill equation (Eq. (2)) was found to provide a better fit to the experimental data ($p < 0.05$, Table 1), indicating that autoactivation does take place. The correlation coefficients (R^2) obtained for the Hill model were closer to unity compared to those with the Michaelis–Menten model (Table 1). The Hill coefficients for S-norketamine and R-norketamine formation were 0.47 and 0.59, respectively. In contrast to the case with CYP3A4, these values are not close to unity. The regression curves for S-norketamine and R-norketamine formation appear to be almost superimposed with that for R-norketamine being lower compared to that for S-norketamine (Fig. 5B) and calculated V_{max} values differ less than 10% (Table 1). It was surprising to realize, that the two curves were found to differ significantly ($p = 0.018$) from a statistical point of view, indicating that N-demethylation of ketamine by CYP2B6 is stereoselective as well. There would be no significant difference if the regression curves would intersect.

Intrinsic clearance (CL_{int}), which defines the rate of metabolism for a given drug concentration, and maximal clearance due to autoactivation (Cl_{max}), which provides an estimate of the highest clearance attained as substrate concentration increases before any saturation of the enzyme sites, were calculated according to $CL_{int} = V_{max}/K_m$ and $Cl_{max} = (V_{max}/K') [(n-1)/n(n-1)^{1/n}]$, respectively [31]. Clearance values are listed in Table 1. The data reveal that the clearance for CYP2B6 is larger compared to CYP3A4. Furthermore, calculated clearance values for the formation of S-norketamine are significantly larger compared to those of R-norketamine in all cases.

3.4. Comparison with in vitro data obtained with HLM

In order to approximate the *in vivo* situation metabolite formation from ketamine incubated with single CYP enzymes was compared to incubations with HLM containing a mixture of enzymes composed of CYP1A2, CYP2A6, CYP2B6, CYP2C8, CYP2C9, CYP2C19, CYP2D6, CYP2E1, CYP3A4, CYP4A and FMO. In incubations of HLM with ketamine and norketamine all metabolites produced by CYP2B6 and CYP2A6 were detected. These data suggest that the detected metabolites are mainly formed from norketamine and not via hydroxylation of ketamine followed by N-demethylation of hydroxyketamine metabolites. Thus, N-demethylation of ketamine is the major metabolic step in man as was previously reported for equines [15].

The kinetic data for the N-demethylation in the presence of HLM, which were assessed with racemic ketamine at 10 different concentrations (6–2000 μM) and having a final protein concentration of 0.5 mg/mL (total CYP content: about 6 pmol/mL) [14], are included in Table 1. Data analysis with both models, Michaelis–Menten and Hill, resulted in reasonable fits. For both enantiomers, the p-values of the F-test were determined to be higher than 0.05 and the Hill coefficients (n) to be close to unity. This suggests that the Michaelis–Menten fit is better, which is in agreement with the results discussed by Kharasch and Labroo [10] and Schmitz et al. [14]. A difference in the N-demethylation rates of the ketamine enantiomers was observed with HLM. Compared to S-norketamine, a smaller amount of R-norketamine was formed which is consistent with our previous findings [14,24]. The formation curves for S- and R-norketamine were found to differ significantly ($p = 0.0003$). Furthermore, clearance for the S-enantiomer was significantly larger compared to the R-enantiomer, which is in agreement with data published by Yanagihara et al. [11]. The clearance values were smaller than those observed for the two single CYPs (Table 1).

4. Conclusions

The enantioselective CE assay for analysis of ketamine and its metabolites in microsomal preparations has been successfully used to identify individual CYP enzymes that are involved in the metabolism of ketamine and norketamine. The findings indicate that a large proportion of the CYP enzymes in the liver are involved in the demethylation of ketamine whereas only two low abundant enzymes metabolize norketamine. To our knowledge, the pre-

sented data are the first which identify enzymes that are involved in biotransformation of norketamine to further metabolites in man. Results from our study reveal norketamine to be the major metabolite resulting from ketamine metabolism. Among the enzymes tested, CYP3A4 and CYP2B6 could be shown to be the major enzymes responsible for the N-demethylation of ketamine. Hijazi and Boulieu [12] observed that a correlation between ketamine N-demethylation activity and CYP3A4- and CYP2B6-specific activities exists in human microsomes. This conclusion is in agreement with our results. For these two enzymes, analysis by enantioselective CE provided the *in vitro* pharmacokinetics of the formation of the norketamine enantiomers in incubations with racemic ketamine. CE is thereby shown to be an attractive approach to elucidate differences in the stereoselectivity in the investigated metabolic steps *in vitro*. Furthermore, CYP2B6 and CYP2A6 were found to be the only CYP enzymes to produce all metabolites found in incubations with ketamine or norketamine and HLM. CYP2B6 was long considered not to be of importance in drug metabolism. New investigations indicate the high relevance of this enzyme in the metabolism of a number of drugs. It particularly catalyzes various oxidative reactions of non-planar, weakly basic and fairly lipophilic compounds with one or two hydrogen bond acceptors [33], such as ketamine [11,12] and methadone [34,35].

Acknowledgement

This work was funded by the Swiss National Science Foundation.

References

[1] R.C. Baselt, R.H. Cravey, Disposition of Toxic Drugs and Chemicals in Man, 4th ed., Chemical Toxicology Institute, Foster City, CA, 1995, p. 412.
[2] A.C. Moffat, M.D. Osselton, B. Widdop, L.Y. Galichet (Eds.), Clarke's Analysis of Drugs and Poisons in Pharmaceuticals, Body Fluids and Postmortem Material, 3rd ed., Pharmaceutical Press, London, UK, 2004, p. 1152.
[3] B. Sinner, B.M. Graf, Handb. Exp. Pharmacol. 182 (2008) 313.
[4] R. Craven, Anaesthesia 62 (2007) 48.
[5] L.C. Mathisen, P. Skjelbred, L.A. Skoglund, I. Oye, Pain 61 (1995) 215.
[6] H.A. Adams, C. Werner, Anaesthesist 46 (1997) 1026.
[7] A. Cromhout, Emerg. Med. 15 (2003) 155.
[8] M.K. Huang, C. Liu, J.H. Li, S.D. Huang, J. Chromatogr. B 820 (2005) 165.
[9] T.F. Woolf, J.D. Adams, Xenobiotica 17 (1987) 839.
[10] E.D. Kharasch, R. Labroo, Anesthesiology 77 (1992) 1201.
[11] Y. Yanagihara, S. Kariya, M. Ohtani, K. Uchino, T. Aoyama, Y. Yamamura, T. Iga, Drug Metab. Dispos. 29 (2001) 887.
[12] Y. Hijazi, R. Boulieu, Drug Metab. Dispos. 30 (2002) 853.
[13] S.C. Turfus, M.C. Parkin, D.A. Cowan, J.M. Halket, N.W. Smith, R.A. Braithwaite, S.P. Elliot, G.B. Steventon, A.T. Kicman, Drug Metab. Dispos. 37 (2009) 1769.
[14] A. Schmitz, W. Thormann, L. Moessner, R. Theurillat, K. Helmja, M. Mevissen, Electrophoresis 31 (2010) 1506.
[15] A. Schmitz, R. Theurillat, P.-G. Lassahn, M. Mevissen, W. Thormann, Electrophoresis 30 (2009) 2912.
[16] J.D. Adams, T.A. Baillie, A.J. Trevor, N. Castagnoli, Biomed. Mass Spectrom. 8 (1981) 527.
[17] A. Schmitz, C.J. Portier, W. Thormann, R. Theurillat, M. Mevissen, J. Vet. Pharmacol. Ther. 31 (2008) 446.
[18] S.A. Savchuk, E.S. Brodskii, B.A. Rudenko, A.A. Formanovskii, I.V. Mikhura, N.A. Davydova, J. Anal. Chem. 52 (1997) 1175.
[19] S. Bolze, R. Boulieu, Clin. Chem. 44 (1998) 560.
[20] Y. Hijazi, C. Bodonian, M. Bolon, F. Salord, R. Boulieu, Br. J. Anaesth. 90 (2003) 155.
[21] D.P.K. Lankveld, B. Driessen, L.R. Soma, P.J. Moate, J. Rudy, C.E. Uboh, P. van Dijk, L.J. Hellebrekers, J. Vet. Pharmacol. Ther. 29 (2006) 477.
[22] R. Theurillat, M. Knobloch, O. Levionnois, P. Larenza, M. Mevissen, W. Thormann, Electrophoresis 26 (2005) 3942.
[23] R. Theurillat, M. Knobloch, A. Schmitz, P.G. Lassahn, M. Mevissen, W. Thormann, Electrophoresis 28 (2007) 2748.
[24] L. Capponi, A. Schmitz, W. Thormann, R. Theurillat, M. Mevissen, Am. J. Vet. Res. 70 (2009) 777.
[25] M.P. Larenza, M.F. Landoni, O.L. Levionnois, M. Knobloch, P.W. Kronen, R. Theurillat, U. Schatzmann, W. Thormann, Br. J. Anaesth. 98 (2007) 204.
[26] M.P. Larenza, M. Knobloch, M.F. Landoni, O.L. Levionnois, P.W. Kronen, R. Theurillat, U. Schatzmann, W. Thormann, Vet. J. 177 (2008) 432.
[27] M. Knobloch, C.J. Portier, O.L. Levionnois, R. Theurillat, W. Thormann, C. Spadavecchia, M. Mevissen, Toxicol. Appl. Pharmacol. 216 (2006) 373.
[28] C. Peterbauer, M.P. Larenza, M. Knobloch, R. Theurillat, W. Thormann, M. Mevissen, C. Spadavecchia, Vet. Anaesth. Analg. 35 (2008) 414.
[29] M.P. Larenza, C. Peterbauer, M.F. Landoni, O.L. Levionnois, U. Schatzmann, C. Spadavecchia, W. Thormann, Am. J. Vet. Res. 70 (2009) 831.
[30] J. Wojcikowski, L. Pichard-Garcia, P. Maurel, W.A. Daniel, Eur. Neuropsychopharmacol. 14 (2004) 199.
[31] J.B. Houston, K.E. Kenworthy, Drug Metab. Dispos. 28 (2000) 246.
[32] T.S. Tracy, M.A. Hummel, Drug Metab. Rev. 36 (2004) 231.
[33] M. Turpeinen, H. Raunio, O. Pelkonen, Curr. Drug Metab. 7 (2006) 705.
[34] J.G. Gerber, R.J. Rhodes, J. Gal, Chirality 16 (2004) 36.
[35] R.A. Totah, P. Sheffels, T. Roberts, D. Whittington, K. Thummel, E.D. Kharasch, Anesthesiology 108 (2008) 363.